



# Triethylenetetramine complexes of cobalt(III) having anion binding sites: synthesis, characterisation, crystal structure, anti-bacterial and anti-cancer properties of $[\text{Co}(\text{trien})(\text{NO}_2)_2]_2\text{Cr}_2\text{O}_7$ and $[\text{Co}(\text{trien})(\text{NO}_2)_2]\text{SCN}$

MONIKA CHETAL<sup>a</sup>, DINESH TALWAR<sup>a,\*</sup>, RAGHUBIR SINGH<sup>a</sup>, SANTOSH ARORA<sup>a</sup>, VIMAL BHARDWAJ<sup>b</sup>, SUBASH CH. SAHOO<sup>c</sup>, RAMAN KUMAR<sup>c</sup> and ROHIT SHARMA<sup>d</sup>

<sup>a</sup>Department of Chemistry, DAV College, Sector-10, Chandigarh 160010, India

<sup>b</sup>Department of Chemistry, Dr. B. R. Ambedkar, National Institute of Technology, Jalandhar 144011, Punjab, India

<sup>c</sup>Department of Chemistry, Panjab University, Chandigarh 160014, India

<sup>d</sup>Department of Microbial Biotechnology, Panjab University, Chandigarh 160014, India

E-mail: dinesh\_talwar58@yahoo.co.in

MS received 8 September 2020; revised 9 November 2020; accepted 17 November 2020

**Abstract.** Crystals of cobalt(III) salts dinitro(triethylenetetramine)cobalt(III) dichromate  $[\text{Co}(\text{trien})(\text{NO}_2)_2]_2\text{Cr}_2\text{O}_7$  (**1**) and dinitro(triethylenetetramine)cobalt(III) thiocyanate  $[\text{Co}(\text{trien})(\text{NO}_2)_2]\text{SCN}$  (**2**) have been synthesized to investigate  $[\text{Co}(\text{trien})(\text{NO}_2)_2]^+$  cation as a promising host to capture dichromate and thiocyanate anions. The characterization of the newly synthesized compounds was accomplished by elemental analysis and spectroscopic techniques (IR, UV/visible and <sup>1</sup>H-NMR) and solubility product measurement. The asymmetric unit of complex **1** has a half dichromate anion and one  $[\text{Co}(\text{trien})(\text{NO}_2)_2]^+$  cation while that of complex **2** has one thiocyanate anion and one  $[\text{Co}(\text{trien})(\text{NO}_2)_2]^+$  cation as divulged by X-ray structure determination. The structural investigation exhibited that the crystal lattice was stabilized by second sphere hydrogen bonding interactions such as N–H<sub>trien</sub>...O (dichromate), C–H<sub>trien</sub>...O (dichromate), N–H<sub>trien</sub>...N (thiocyanate) and C–H<sub>trien</sub>...N (thiocyanate) interactions resulting in the formation of supramolecular assemblies. The complexes **1** and **2** were further examined for antibacterial activity and the findings unveiled moderate activity against gram-negative bacteria such as *Escherichia coli* and *Pseudomonas aeruginosa* species. These complexes were also scrutinized for anti-proliferative activity against malignant PANC-1 cells using MTT cell survival analysis. Complex **1** exhibited remarkable anticancer activity whereas complex **2** has comparatively lesser anticancer potential.

**Keywords.** Cobalt(III); second sphere coordination; dichromate; thiocyanate; antibacterial; anticancer.

## 1. Introduction

Anion binding is an important area of supramolecular chemistry due to fascinating applications of anions in diverse fields.<sup>1–3</sup> Anions play a crucial role in maintaining our lives because they actively take part in many enzymatic and biochemical reactions.<sup>4,5</sup> However, dysregulation of some anions results in serious maladies such as cystic fibrosis and epilepsy.<sup>6,7</sup> Keeping in view the beneficial and detrimental effects of anions, their recovery is of utmost importance.

Hence earnest attention must be paid towards the design and synthesis of artificial receptors which can capture specific anions.

Authentic capturing of anions is really an arduous task due to some exigencies like-greater size and low charge to size ratio of anions in comparison to iso-electronic cations, substantial diversity in their shapes and geometries and their pH sensitivity.<sup>8</sup> In the past decades, anion receptors having organic functionalities such as ammonium, amide, urea, thiourea, calixpyrrole, calixarene, guanidinium and pyridinium were

\*For correspondence

Electronic supplementary material: The online version of this article (<https://doi.org/10.1007/s12039-020-01877-z>) contains supplementary material, which is available to authorized users.

utilized.<sup>9–16</sup> The biggest drawback of the organic ligands was that their geometry cannot be suitably oriented for the successful binding of anions. This predicament can be conquered by complexing these organic ligands with the transition metals leading to proper interaction with the anions. The focus of the present work is on the preparation of cobalt(III) complexes containing triethylenetetramine which behave as second sphere coordinating unit for binding with the anion.  $[\text{Co}(\text{trien})(\text{NO}_2)_2]^+$  cation behaves as a good anion receptor owing to its peculiar attributes like six N–H and twelve C–H hydrogen bond donor groups, unipositive charge for electrostatic interactions and an apt structural architecture for capturing the anions.

Dichromate and thiocyanate anions particularly grab our attention owing to their manifold applications in diverse fields. Dichromates are utilized in leather tanning, photography, catalysis, wood staining, chrome plating and in the textile industry.<sup>17,18</sup> However, these hexavalent chromium compounds are toxic as well as carcinogenic and harm reproductive health by acting as mutagenic agents.<sup>19</sup> Thiocyanate has worthwhile therapeutic properties as it can act as an anti-sickling agent and anti-oxidant agent.<sup>20,21</sup> On the flip side, thiocyanate inhibits the sodium iodide symporter, preventing the accumulation of iodides in the thyroidal system.<sup>22</sup> Hence, systematized investigation of binding of these significant anions with some synthetic setup is crucial. Under this backdrop, this paper focuses on the synthesis, spectroscopic and crystallographic characterization along with the antibacterial and anti-proliferative investigation of  $[\text{Co}(\text{trien})(\text{NO}_2)_2]_2\text{Cr}_2\text{O}_7$  and  $[\text{Co}(\text{trien})(\text{NO}_2)_2]\text{SCN}$ . As many cobalt complexes were found to have antimicrobial and anticancer properties,<sup>23–25</sup> antibacterial potency of complex **1** and **2** were scrutinized against four different microbes- *Escherichia coli*, *Pseudomonas aeruginosa*, *Staphylococcus aureus* and *Enterococcus hirae* by using agar well diffusion method. Their anticancer potential was scrutinized against PANC-1 cells by using MTT cell survival colorimetric analysis.

## 2. Experimental

### 2.1 Materials

All the required chemicals namely cobalt(II) chloride hexahydrate (Merck), sodium nitrite (LobaChemie), triethylenetetramine (SigmaAldrich), potassium dichromate (LobaChemie), ammonium thiocyanate (LobaChemie) and concentrated hydrochloric acid

(LobaChemie) were purchased and used without being further purified. All the reactions were accomplished without excluding oxygen and water.

### 2.2 Synthesis

**2.2a Synthesis of  $[\text{Co}(\text{trien})(\text{NO}_2)_2]\text{Cl}$ :** The starting material  $[\text{Co}(\text{trien})(\text{NO}_2)_2]\text{Cl}$  was prepared by reacting  $\text{CoCl}_2 \cdot 6\text{H}_2\text{O}$ ,  $\text{NaNO}_2$ , triethylenetetramine (trien) and conc. HCl by adopting the reported procedure.<sup>26</sup> The dissolution of  $\text{CoCl}_2 \cdot 6\text{H}_2\text{O}$  (11.9 g, 0.05 mmol) and  $\text{NaNO}_2$  (7.25 g, 0.1 mmol) in 10 mL distilled water was accomplished in a side-arm flask. This flask was then placed in an ice bath. Another solution was prepared by dissolving 7.44 mL (0.05 mmol) of triethylenetetramine in 10 mL of deionized water, into which 4.4 mL (0.1 mmol) of conc. HCl was added. Then this solution was poured into cobalt chloride - sodium nitrite solution and the reaction mixture was aerated for 90 min in an ice bath. The brown colored precipitates obtained were filtered and recrystallized from hot water. Characterization of the desired product was consistent with its structure (Figures S7 and S8, Supplementary Information). FT-IR ( $\text{cm}^{-1}$ ): 3223 (m) for  $\nu_{as}(\text{NH}_2)$ , 3115 (m) for  $\nu_s(\text{NH}_2)$ , 1402 (s) for  $\nu_{as}(\text{NO}_2)$ , 1346 (s) for  $\nu_s(\text{NO}_2)$ , 1058 (m) for  $\nu(\text{C}-\text{N})$ , 478 (m) for  $\nu(\text{Co}-\text{N})$ .  $^1\text{H-NMR}$  ( $\text{DMSO}-d_6$ , ppm): {6.36 (s, 2H), 5.69 (s, 2H), 4.92 (s, 2H) NH}, 3.40 (s, 2H ( $\text{CH}_2$ )), 2.84 (m, 10H ( $\text{CH}_2$ )).

**2.2b Synthesis of  $[\text{Co}(\text{trien})(\text{NO}_2)_2]_2\text{Cr}_2\text{O}_7$  (**1**):** 0.9975 g (0.1 mmol) of  $[\text{Co}(\text{trien})(\text{NO}_2)_2]\text{Cl}$  was dissolved in 30 mL of hot distilled water. After cooling it to room temperature, an aqueous solution of 0.2206 g (0.05 mmol) of  $\text{K}_2\text{Cr}_2\text{O}_7$  in 15 mL of distilled water was added to it. Then the resulting solution was kept in the refrigerator. Needle shaped orange colored crystals started appearing after 8 h. The crystals were separated from the mother liquor by filtration, washed with cold water and dried in a desiccator. Yield = 80%. The elemental analysis is consistent with the composition  $[\text{Co}(\text{trien})(\text{NO}_2)_2]_2\text{Cr}_2\text{O}_7$ . For  $\text{C}_{12}\text{H}_{36}\text{Co}_2\text{Cr}_2\text{N}_{12}\text{O}_{15}$  (Found: (%) C, 18.00; H, 4.439; N, 20.881; Calculated: (%) C, 17.78; H, 4.44; N, 20.741. FT-IR ( $\text{cm}^{-1}$ ): 3212 (m) for  $\nu_{as}(\text{NH}_2)$ , 3125(m) for  $\nu_s(\text{NH}_2)$ , 3236(m) for  $\nu(\text{NH})$ , 1405 (s) for  $\nu_{as}(\text{NO}_2)$ , 1347 (s) for  $\nu_s(\text{NO}_2)$ , 1059 (m) for  $\nu(\text{C}-\text{N})$ , 951 (s) for  $\nu(\text{Cr}-\text{O})$ , 790 (m) for  $\nu(\text{Cr}-\text{O}-\text{Cr})$ , 482 (w) for  $\nu(\text{Co}-\text{N})$ .  $^1\text{H-NMR}$  ( $\text{DMSO}-d_6$ , ppm): {5.82 (s, 2H), 5.31 (s, 2H), 5.01 (s, 2H) NH}, 3.39 (s, 2H ( $\text{CH}_2$ )), 2.84 (m, 10H, ( $\text{CH}_2$ )). UV-Visible spectrum in

water ( $\lambda$ ): 328 nm. Solubility in water: 0.935 g/100 g at 25 °C.  $K_{sp} = 5.786 \times 10^{-6}$ .

**2.2c Synthesis of  $[Co(trien)(NO_2)_2]SCN$  (2):** dinitro(triethylenetetramine)cobalt(III) chloride (0.99 g, 0.1 mmol) was dissolved in 30 mL of hot distilled water. An aqueous solution of ammonium thiocyanate (0.11 g, 0.1 mmol) in 15 mL distilled water was added to it. The resultant solution thus obtained was cooled in the refrigerator. Brown colored crystals began to develop on third day. Separation of crystals from mother liquor was accomplished by filtration. After giving washing with cold water, crystals were placed in a desiccator for drying. Yield = 75%. The elemental analysis was in agreement with the composition  $[Co(trien)(NO_2)_2]SCN$ . For  $C_7H_{18}CoN_7O_4S$  (Found: (%) C, 23.74; H, 5.00; N, 27.38; Calculated: (%) C, 23.66; H, 5.07; N, 27.60) Solubility in water: 1.385 g/100 g at 25 °C.  $K_{sp} = 1.521 \times 10^{-3}$ . FT-IR (KBr pellet,  $cm^{-1}$ ): 3235 (sh) for  $\nu(NH)$ , 3212(s) for  $\nu_{as}(NH_2)$ , 3127(s) for  $\nu_s(NH_2)$ , 2065 (s) for  $\nu(SCN)$ , 1405(s) for  $\nu_{as}(NO_2)$ , 1346(s) for  $\nu_s(NO_2)$ , 1060 (m) for  $\nu(C-N)$ , 820 (w) for  $\nu(NCS)$ , 481 (w) for  $\nu(Co-N)$ .  $^1H$ -NMR (DMSO- $d_6$ , ppm): {5.79 (s, 2H), 5.31 (s, 2H), 5.02 (s, 2H) NH}, 3.35 (m, 2H), 2.80 (m, 10H). UV-Visible spectrum in water ( $\lambda$ ): 242 nm and 322 nm.

### 2.3 Physical measurements

Automatic PERKIN ELMER 2400 CHN elemental analyzer was utilized to estimate C, H and N. BRUKER Spectrum RXFT-IR system was used to record FTIR spectrum with the help of KBr pellets. EI double beam UV-visible spectrophotometer was employed to record UV/visible spectrum. Bruker Advanced Neo 500 MHz NMR Spectrometer was utilized to record the  $^1H$  NMR spectrum at 25 °C in DMSO- $d_6$ . The chemical shift values ( $\delta$ ) in ppm were expressed downfield from TMS (tetramethylsilane) taken as an internal standard.

**2.3a Single-crystal x-ray crystallography:** A Bruker SMART APEX CCD diffractometer was utilized to garner single-crystal X-ray data at 300 K with the help of Mo  $K_{\alpha}$  radiation ( $\lambda = 0.71073 \text{ \AA}$ ) monochromated by graphite. OLEX2 or WINGX package with the help of SHELXS-97 was utilized to solve the crystal structures and the refinement of the structures was accomplished by using SHELXL-97.<sup>27</sup> The refinement of all non-hydrogen atoms was done anisotropically. Hydrogen atoms were fixed at

geometrically calculated positions and were refined using the riding model.

**2.3b Antibacterial assay:** Agar well diffusion method was utilized for the antibacterial screening of complex **1** and **2**. Bacterial strains for antibacterial assay were procured from MTCC, IMTECH, Chandigarh, India. Bactericidal potential of complexes was examined against four bacterial strains namely *Escherichia coli* (MTCC 2961), *Staphylococcus aureus* (MTCC 3160), *Pseudomonas aeruginosa* (MTCC 424), and *Enterococcus hirae* (MTCC 2728).

Briefly, *E. coli*, *S. aureus* and *P. aeruginosa* were grown in nutrient broth and *E. hirae* was grown in trypticase soya broth overnight at 37 °C. The adjustment of a bacterial load to  $10^4$  colony-forming units per mL was brought about with the help of spectrophotometer at absorbance 600 nm. 100  $\mu$ L of  $10^4$  cfu/mL bacterial culture was spread onto the respective media Petri plates for each bacterial strain. 5 mg of each of the complexes was dissolved in 1 mL of autoclaved type 1 water and 100  $\mu$ L of the solution was poured into the wells punched in the agar plate. 5  $\mu$ L of antibiotic Rifampicin at a concentration of 2 mg/mL was considered as the positive control and the same volume of a solvent having no complex was used as a negative control.

The four plates, thus prepared for the four bacterial strains were incubated at 37 °C for 24 h. After the incubation period, the antibacterial activity of complex **1** and **2** was noticed by measuring the diameter of the zone of inhibition in millimetres with reference to the antibiotic Rifampicin.

**2.3c Cytotoxic activity:** Cell lines and growth medium

- 1. PANC-1** The pancreatic cancer cell line, PANC-1 was procured from the National Centre for Cell Sciences (NCCS), Pune. The cells were cultivated in DMEM medium (Dulbecco's Modified Eagles medium) supplemented with 10% fetal bovine serum (FBS), 100 U/mL Penicillin, 100  $\mu$ g/mL Streptomycin, and 0.25  $\mu$ g/mL Amphotericin B.
- 2. hTERT-HPNE** The normal, non-cancerous pancreatic cell line, hTERT-HPNE (ATCC<sup>®</sup> CRL-4023<sup>TM</sup>) was procured from American Type Culture Collection (Manassas, US). The cells were cultivated in base medium: DMEM without glucose (Gibco) supplemented with 5% FBS (Gibco), 10 ng/mL human recombinant EGF (Sigma), 5.5 mM D-glucose (1g/L) (Gibco), 2mM L-glutamine (Gibco), 1.5 g/L sodium

bicarbonate (Gibco) and 25% Medium M3 base (Incell Corp.).

### 3. MTT Cytotoxicity assay

The *in vitro* anticancer screening of complex **1** and **2** was accomplished by employing MTT cytotoxicity assay. Briefly,  $10^4$  cells per well were seeded in a 96 well culture plate. The cells were treated with different concentrations of complexes for 24 h at 37 °C and 5% CO<sub>2</sub> supply in a humidified incubator. The medium was replaced after the treatment and 20 μL of MTT solution (5 mg/mL) was poured into each well followed by incubation for 4 h at 37 °C. Thereafter, the medium was removed and 100 μL of DMSO was added to dissolve the formazan crystals. The experiment was repeated thrice and the medium without complex was treated as control. Multiskan FC Microplate photometer of Thermo Fisher Scientific brand was used to record the absorbance at 570 nm.<sup>28</sup>

The cell viability was determined by the breakdown of a tetrazolium salt into purple-coloured insoluble formazan crystals.<sup>29,30</sup> This cleavage of tetrazolium compound takes place only in active mitochondria of living cells. The viable cells convert the yellowish MTT dye to purple coloured formazan crystals. The percentage of survival was calculated by proportioning the absorbance recorded from a test sample to that of the control group as follows:

$$\% \text{ age Cell Survival} = \frac{A_{\text{Test}} - A_{\text{Blank}}}{A_{\text{Control}} - A_{\text{Blank}}} \times 100$$

Here  $A_{\text{test}}$ ,  $A_{\text{control}}$  and  $A_{\text{blank}}$  are the mean absorbance of treated cells, untreated cells and medium blank respectively. The results were expressed as Mean  $\pm$  SD of percentage cell survival.

A *concentration versus percentage survival* graph was plotted for the complex **1** and **2** and IC<sub>50</sub> for each was determined. IC<sub>50</sub> is that concentration of the complex at which the survival of the cancer cells is reduced to 50% of the control cells. Lower the IC<sub>50</sub>, greater is the efficacy of the complex. The complex showing the significant activity at lower IC<sub>50</sub> was studied for its safety on the normal cell line i.e., hTERT-HPNE.

## 3. Results and Discussion

### 3.1 Synthesis

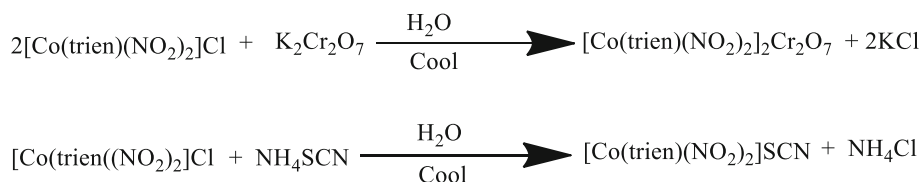
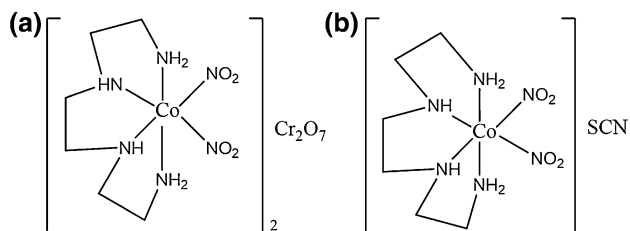
Synthesis of [Co(trien)(NO<sub>2</sub>)<sub>2</sub>]Cl was accomplished by the reaction of Co(II) salt with one equivalent of triethylenetetramine (tetradentate ligand) and two

equivalents of sodium nitrite in water. Atmospheric air was utilized for the oxidation of Co(II) salt. The intermixing of [Co(trien)(NO<sub>2</sub>)<sub>2</sub>]Cl and potassium dichromate in 2:1 ratio resulted in the synthesis of complex **1**. Complex **2** was synthesized by intermixing of [Co(trien)(NO<sub>2</sub>)<sub>2</sub>]Cl and ammonium thiocyanate in 1:1 ratio. Single crystals of complex **1** and **2** were successfully isolated and subjected to X-Ray crystallographic analysis in order to establish the structure. The characterization of newly synthesized complexes was done by elemental analysis, FT-IR, <sup>1</sup>H-NMR and UV-Visible spectral studies (Scheme 1).

**3.1a Spectral characterization of complex 1:** The assignment of peaks has been carried out on the basis of previous literature reports.<sup>31</sup> IR peaks at 3212 cm<sup>-1</sup> and 3125 cm<sup>-1</sup> correspond to asymmetric and symmetric stretching of N–H (amino group). A very weak peak in the form of shoulder band appears at 3236 cm<sup>-1</sup> due to N–H stretching vibrations of a secondary amino group (Figure S1, Supplementary Information). These values of N–H stretching are lower than the base value (3300–3500 cm<sup>-1</sup>) due to the involvement of NH<sub>2</sub> and NH groups in extensive H-bonding with the dichromate ion. However, peaks at 1405 cm<sup>-1</sup> and 1347 cm<sup>-1</sup> correspond to asymmetric and symmetric stretching of NO<sub>2</sub> groups. IR peak at 1059 cm<sup>-1</sup> arises due to C–N stretching. IR peaks at 951 cm<sup>-1</sup> is due to stretching vibrations of Cr–O bonds of Cr<sub>2</sub>O<sub>7</sub><sup>2-</sup> anion whereas peak at 790 cm<sup>-1</sup> is due to Cr–O–Cr vibrations of this anion.<sup>32</sup> Co–N bond is indicated by IR band at 482 cm<sup>-1</sup>.<sup>33</sup>

<sup>1</sup>H-NMR spectra of the newly synthesized complex salt are recorded in DMSO-*d*<sub>6</sub>. There are three singlets for the N–H protons at  $\delta$  5.01, 5.31 and 5.82 ppm with the intensity ratio 2:2:2 (Figure S2, Supplementary Information). All the CH<sub>2</sub> absorptions in this complex appear up field than the NH absorptions. A singlet at 3.39 ppm belongs to two protons of central ethylene linkages based on the multiplicity and symmetry considerations. The protons of terminal ethylene linkages as well as remaining protons of the central ring must overlap to form a complex multiplet at 2.84 ppm (Scheme 2).<sup>34,35</sup>

The electronic spectrum of the newly synthesized salt was recorded in water in order to elucidate the kinds of electronic transitions (Figure S3, Supplementary Information). For low spin octahedral Co(III) complexes, two types of spin allowed singlet to singlet *d-d* transitions are expected i.e. <sup>1</sup>A<sub>1g</sub> → <sup>1</sup>T<sub>1g</sub> (low energy) and <sup>1</sup>A<sub>1g</sub> → <sup>1</sup>T<sub>2g</sub> (high energy). In complex **1**, the electronic transition was observed at 328 nm.<sup>36</sup>

**Scheme 1.** Schematic representation of chemical reactions.**Scheme 2.** (a) Structure of  $[\text{Co}(\text{trien})(\text{NO}_2)_2]_2\text{Cr}_2\text{O}_7$ . (b) Structure of  $[\text{Co}(\text{trien})(\text{NO}_2)_2]\text{SCN}$ .

**3.1b Spectral characterization of complex 2:** The FT-IR peaks are assigned by consulting previous reports of literature.<sup>31</sup> IR peaks at  $3212\text{ cm}^{-1}$  and  $3127\text{ cm}^{-1}$  arises due to asymmetric and symmetric stretching of N–H (amino group). N–H stretching vibrations of the secondary amino group appear in the form of shoulder band at  $3235\text{ cm}^{-1}$  (Figure S4, Supplementary Information). These N–H stretching values are lesser than the base value ( $3300\text{--}3500\text{ cm}^{-1}$ ) as  $\text{NH}_2$  and  $\text{NH}$  groups are involved in extensive H-bonding with the thiocyanate ion. However, peaks due to asymmetric and symmetric stretching vibrations of  $\text{NO}_2$  groups appear at  $1405\text{ cm}^{-1}$  and  $1346\text{ cm}^{-1}$ , respectively. IR peak at  $1060\text{ cm}^{-1}$  corresponds to C–N stretching. IR peak at  $2065\text{ cm}^{-1}$  appears due to stretching vibrations of C–N bond of SCN anion whereas peak at  $820\text{ cm}^{-1}$  is formed due to C–S vibrations of this anion.<sup>37</sup> IR band at  $481\text{ cm}^{-1}$  corresponds to Co–N bond.<sup>33</sup>

<sup>1</sup>H-NMR spectrum of complex **2** is recorded in  $\text{DMSO-}d_6$ . Three singlets corresponding to N–H protons appear at  $\delta$  5.79, 5.31 and 5.02 ppm with the intensity ratio 2:2:2 (Figure S5, Supplementary Information). In comparison to NH absorptions, all the  $\text{CH}_2$  absorptions in this complex appear up field. A multiplet at 3.35 ppm is assigned to two protons of central ethylene linkages on the basis of multiplicity and symmetry considerations. The remaining protons of the central ring and the protons of terminal ethylene linkages must overlap to form a complex multiplet at 2.80 ppm.<sup>34,35</sup>

The UV-visible spectrum of the complex **2** was recorded in water for the elucidation of kinds of electronic transitions (Figure S6, Supplementary

Information). Two kinds of spin allowed singlet to singlet  $d\text{-}d$  transitions are expected in low spin octahedral Co(III) complexes i.e.  ${}^1\text{A}_{1g} \rightarrow {}^1\text{T}_{1g}$  (low energy) and  ${}^1\text{A}_{1g} \rightarrow {}^1\text{T}_{2g}$  (high energy). The electronic transitions were observed at 242 nm and 322 nm in complex **2**.<sup>36</sup>

### 3.2 Solubility product evaluation

Solubility product ( $K_{\text{sp}}$ ) of title complex **1** was determined in the water at  $25\text{ }^\circ\text{C}$ . Solubility measurements indicated that the title complex was sparingly soluble in water while  $[\text{Co}(\text{trien})(\text{NO}_2)_2]\text{Cl}$  has comparatively high solubility. The solubility product of complex **1** was found to be  $5.786 \times 10^{-6}$  while that of  $[\text{Co}(\text{trien})(\text{NO}_2)_2]\text{Cl}$  was measured as  $5.919 \times 10^{-2}$ . It is inferred from this measurement that the complex cation has greater endearment for dichromate ion as compared to chloride ion. The great affinity between cation and dichromate anion might be due to hydrogen bonding interaction between them.

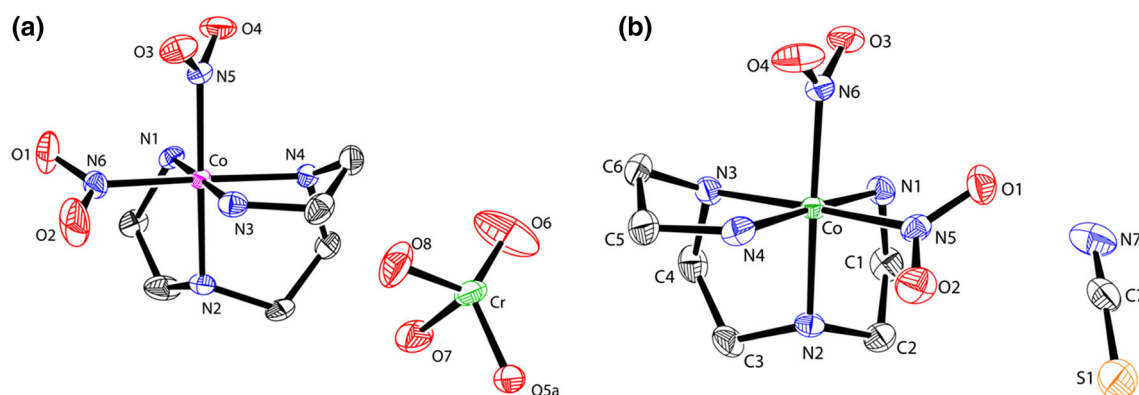
Solubility product determination of complex **2** was accomplished in the water at  $25\text{ }^\circ\text{C}$ . As indicated by solubility measurements, this complex was sparingly soluble in water whose solubility is lesser than that of the starting material  $[\text{Co}(\text{trien})(\text{NO}_2)_2]\text{Cl}$ . The solubility product of complex **2** was found to be  $1.521 \times 10^{-3}$  while that of  $[\text{Co}(\text{trien})(\text{NO}_2)_2]\text{Cl}$  was measured as  $5.919 \times 10^{-2}$ . This measurement discerned that the complex cation has a greater affinity for thiocyanate ion in comparison to chloride ion. Hydrogen bonding interactions might be responsible for this great fondness between cation and thiocyanate anion.

### 3.3 Coordination geometry and packing

**3.3a Elucidation of crystal structure:** The crystal structure of complex **1** discloses that it crystallizes in monoclinic crystal system with  $P2_1/c$  space group (Table 1). In the asymmetric unit of complex **1**, there are one  $[\text{Co}(\text{trien})(\text{NO}_2)_2]^+$  and half of  $\text{Cr}_2\text{O}_7^{2-}$  unit (Figure 1a). The co-ordination environment of Co(III) was occupied by six nitrogen atoms, four from triethylenetetramine ligand and two from nitro

**Table 1.** Crystal data, data collection and refinement parameters of complexes **1** and **2**.

CCDC	1951784	2014888
Empirical formula	C <sub>12</sub> H <sub>36</sub> Co <sub>2</sub> Cr <sub>2</sub> N <sub>12</sub> O <sub>15</sub>	C <sub>7</sub> H <sub>18</sub> CoN <sub>7</sub> O <sub>4</sub> S
<i>M</i> (g mol <sup>-1</sup> )	810.39	355.27
<i>T</i> /K	296	296
$\lambda$ (Å)	0.71073	0.71073
Crystal system	Monoclinic	Orthorhombic
Space group	P2 <sub>1</sub> /c	P2 <sub>1</sub> 2 <sub>1</sub> 2 <sub>1</sub>
<i>a</i> /Å	13.1680 (5)	7.547(5)
<i>b</i> /Å	8.9494 (4)	12.073(5)
<i>c</i> /Å	12.5557 (5)	15.464(5)
$\alpha$ /°	90	90.000(5)
$\beta$ /°	96.2871 (5)	90.000(5)
$\gamma$ /°	90	90.000(5)
<i>V</i> /Å <sup>3</sup>	1470.74 (10)	1409.0(12)
<i>Z</i>	2	4
$\rho_{\text{calc}}$ /g cm <sup>-3</sup>	1.830	1.6746
$\mu$ /mm <sup>-1</sup>	1.912	1.391
<i>F</i> (000)	828.0	738.2
Crystal size/mm <sup>3</sup>	0.4 × 0.4 × 0.3	0.4 × 0.4 × 0.3
Unique reflections	3649	3477
<i>R</i> (int)	0.0350	0.0311
GOF on <i>F</i> <sup>2</sup>	1.057	1.093
<i>R</i> 1 [ <i>I</i> ≥ 2σ( <i>I</i> )]	0.0487	0.0224

**Figure 1.** (a) Asymmetric unit ORTEP diagram of complex **1**. H-atoms and disordered O-atom of the Cr<sub>2</sub>O<sub>7</sub><sup>2-</sup> anion has been removed for clarity. (b) ORTEP diagram of complex **2** with 40% probability. H-atoms have been removed for clarity.

groups (attached cis to the metal center). The complex is a cation where Co(III) central metal ion adopts a distorted octahedral geometry with the extent of distortion of 4.63 degree from ideal value 90° for N1–Co1–N2 bond angle (Table 2). The average bond lengths Co–N (trien), Co–N (NO<sub>2</sub>) are 1.958 and 1.92 Å, respectively, which are close to the reported structures.<sup>38–41</sup>

The triethylenetetramine ligand acts as a tetradentate ligand and co-ordinated to central metal ion occupying three equatorial and one axial site. Other two sites (one equatorial, one axial) are occupied by nitro groups. Few O-atoms of the dichromate (Cr<sub>2</sub>O<sub>7</sub><sup>2-</sup>)

anion found to be disordered and appropriate disordered model has been applied based on the available electron density. The crystal lattice was stabilized by weak non-covalent interactions of N–H⋯O (2.033 Å) and C–H⋯O (2.553 Å) between amine groups and methylene groups of triethylenetetramine with oxygen atoms of dichromate anion respectively (Table 3 and Figure 3a). Along the *b*-axis, the complex **1** showed a layer like arrangement of the [Co(trien)(NO<sub>2</sub>)<sub>2</sub>]<sup>+</sup> moieties in opposite directions (along *c*-axis) where the dichromate ions were sandwiched between the two layers of cations resulting a 2D sheet-like pattern (Figure 2b).

**Table 2.** Selected bond lengths (Å) and bond angles (°) for complexes **1** and **2**.

Atoms	Bond distances (Å)	Atoms	Bond distances (Å)
<i>Complex 1</i>			
Co1 N2	1.971(3)	Cr1 O5B	1.495(6)
Co1 N5	1.914(3)	Cr1 O7B	1.866(7)
Co1 N6	1.925(3)	Cr1 O6	1.490(4)
Co1 N4	1.952(3)	Cr1 O5A	1.866(7)
Co1 N3	1.960(3)	Cr1 O5A	1.686(7)
Co1 N1	1.950(3)	Cr1 O8	1.582(3)
Atoms	Bond angles (°)	Atoms	Bond angles (°)
<i>Complex 1</i>			
N3 Co1 N2	87.33(11)	N1 Co1 N3	93.96(12)
N5 Co1 N2	175.94(13)	O8 Cr1 O7B	97.8(3)
N5 Co1 N6	88.89(12)	O8 Cr1 O7B	97.8(3)
N5 Co1 N4	90.00(13)	O8 Cr1 O5A	108.6(3)
N5 Co1 N3	91.33(12)	O8 Cr1 O5A	99.8(2)
N5 Co1 N1	90.90(13)	O5B Cr1 O8	116.2(3)
N6 Co1 N2	92.71(12)	O5B Cr1 O7B	59.2(4)
N6 Co1 N4	90.59(13)	O5B Cr1 O5A	102.5(3)
N6 Co1 N3	176.09(14)	O7B Cr1 O5A	159.1(3)
N6 Co1 N1	89.93(13)	O6 Cr1 O8	117.6(3)
N4 Co1 N2	93.71(12)	O6 Cr1 O5B	121.2(4)
N4 Co1 N3	85.51(13)	O6 Cr1 O7B	91.7(4)
N1 Co1 N4	178.96(11)	O6 Cr1 O5A	130.4(4)
N1 Co1 N2	85.37(12)	O6 Cr1 O5A	90.0(3)
N1 Co1 N3	93.96(12)	O5ACr1O5A	64.5(3)
O8 Cr1 O7B	97.8(3)		
Atoms	Bond distances (Å)	Atoms	Bond distances (Å)
<i>Complex 2</i>			
Co N4	1.9521(15)	Co N2	1.9579(14)
Co N1	1.9590(14)	Co N6	1.9255(15)
Co N5	1.9144(16)	S C7	1.636(2)
Co N3	1.9725(16)	N7 C7	1.156(3)
Atoms	Bond angles (°)	Atoms	Bond angles (°)
<i>Complex 2</i>			
N1 Co N4	177.86(6)	N2 Co N3	87.85(6)
N5 Co N4	90.63(6)	N6 Co N4	90.57(6)
N5 Co N1	89.85(6)	N6 Co N1	91.53(6)
N3 Co N4	85.31(6)	N6 Co N5	88.70(5)
N3 Co N1	94.20(6)	N6 Co N3	91.76(6)
N3 Co N5	175.91(6)	N6 Co N2	176.65(6)
N2 Co N4	92.72(5)	O2 N5 O1	120.50(14)
N2 Co N1	85.18(5)	O3 N6 O4	119.08(14)
N2 Co N5	91.92(5)	N7 C7 S1	177.86(19)

On the other hand, the crystal structure of complex **2** reveals that it crystallizes in an orthorhombic crystal system of  $P2_12_12_1$  space group (Table 1). In the asymmetric unit of **2**, there is one  $[\text{Co}(\text{trien})(\text{NO}_2)_2]^+$  cationic unit per  $\text{SCN}^-$  anionic unit (Figure 1b). Cationic component of the complex **2** is almost similar to complex **1** and only differs by the  $\text{SCN}^-$  counter ion.

Out of six nitrogen atoms coordinated to central metal ion, four were from triethylenetetramine ligand and two from the nitro groups (attached cis to the metal center). In the complex **2**, Co(III) central metal ion adopts a distorted octahedral geometry with the extent of distortion of 4.88 degrees from ideal value  $90^\circ$  for N2–Co1–N1 bond angle (Table 2). The average bond

lengths Co–N (trien) and Co–N (NO<sub>2</sub>) are 1.96 and 1.92 Å respectively, which are close to the reported structures.

The crystal lattice was stabilized by weak non-covalent interactions of N3–H3...N7 (2.205 Å) and N1–

H1a...N7 (2.243 Å) between the amine group and thiocyanate nitrogen atom (Table 3 and Figure 3b). There is another weak non-covalent interaction between amine and oxygen atoms of nitro groups of N4–H4a...O3 (2.105 Å) and N2–H2...O4 (2.056 Å) and extends the molecules along *b*-axis. Along the *bc*-plan, the complex **2** shows a lamellar like arrangement of the [Co(trien)(NO<sub>2</sub>)<sub>2</sub>]<sup>+</sup> groups where the thiocyanate ions were sandwiched between the cationic layers resulting in a 2D sheet-like pattern (Figure 2d).

**Table 3.** Hydrogen bonding parameters (Å and °) of complexes **1** and **2**.

D–H...A	H...A/Å	D...A/Å	< D–H...A/°
<i>Complex 1</i>			
N4–H4B...O6	2.033	2.869(6)	155.92
N1–H1B...O2	2.140	3.001 (4)	162.46
N1–H1A...O3	2.120	2.983 (4)	154.47
N3–H3...O1	2.074	2.989 (4)	163.01
<i>Complex 2</i>			
D–H...A	H...A/Å	D...A/Å	< D–H...A/°
N3–H3...N7	2.205	3.032(2)	150.76
N1–H1A...N7	2.243	3.082(3)	154.99
N4–H4A...O3	2.105	2.991(2)	167.87
N2–H2...O4	2.056	2.912(2)	156.15

### 3.4 Antibacterial activity

**3.4a Agar well diffusion method:** The screening of antibacterial activity of complex **1** and **2** was done with the help of Agar well diffusion method. The diffusion of complex **1** and **2** into the nutrient agar and trypticase soya agar medium through the wells, inhibited the growth of the microbial strains in that region, creating the zone of inhibition.

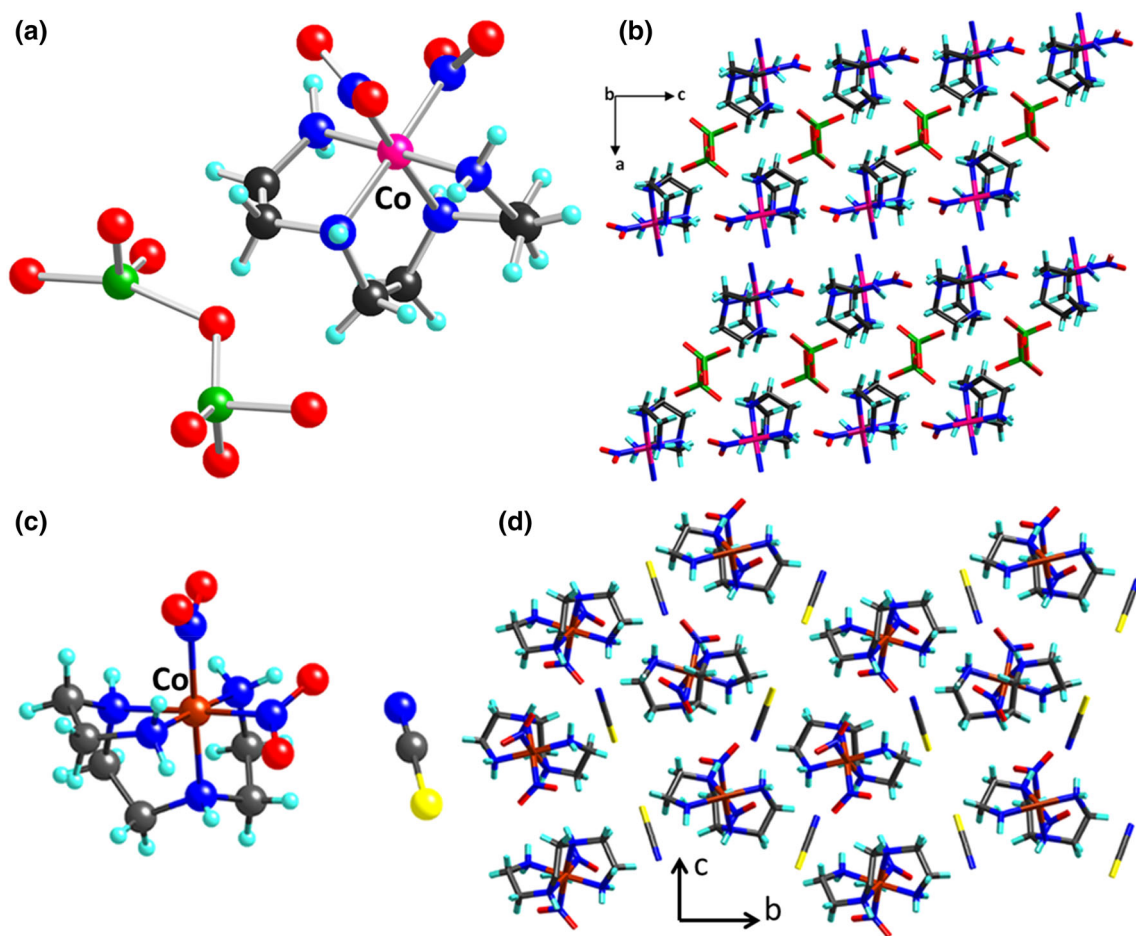


**Figure 2.** (a) Ball and stick model of complex **1** and the disordered O-atoms of the Cr<sub>2</sub>O<sub>7</sub><sup>2-</sup> anion have not shown for clarity. (b) Packing diagram of complex **1** along *b* axis. (c) Ball and stick model of complex **2**. (d) Packing diagram of complex **2** along *bc*-plan. Blue: N; Red: O; Black: C; Sky blue: H; Green: Cr; Yellow: S.

It was discerned that complex **1** and **2** inhibited the growth of gram negative bacteria such as *E. coli* and *P. aeruginosa* with the zone of inhibition having diameter 20.6 mm, 19 mm and 20 mm, 18.3 mm respectively. However, these did not have any antibacterial activity against gram positive bacteria such as *S. aureus* and *E. hirae*. The diameter of zone of inhibition of both the complexes as well as of drug is shown in Table 4.

No zone of inhibition was shown by the solvent control. The impressive antibacterial potency of Co(III) complex is due to its high lipophilic nature. The coordination of metal ion with chelating ligands

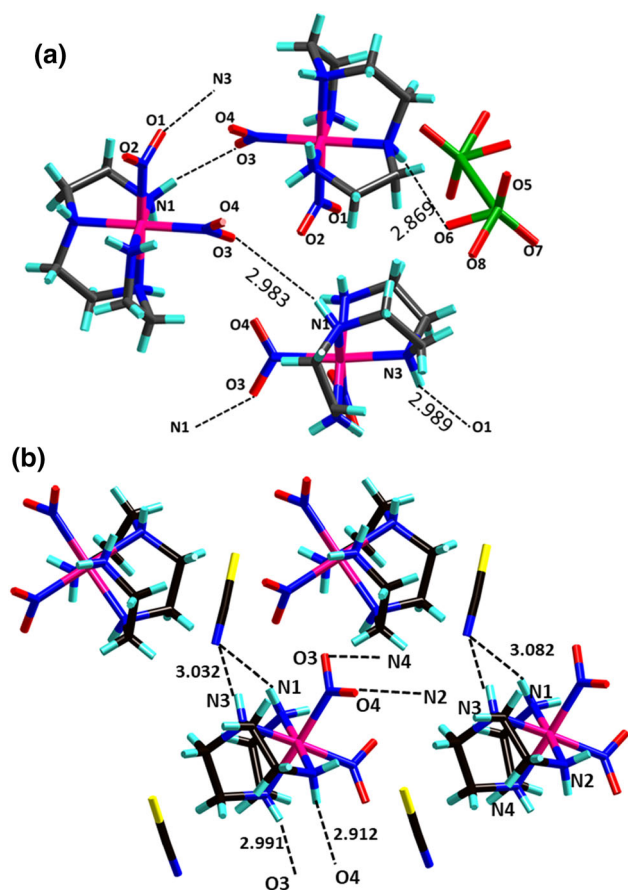


**Figure 3.** Hydrogen bonding interactions (a) between the amine, dichromate and nitro group in complex **1**. (b) between the amine, thiocyanate and nitro group in complex **2**.

results in a reduction of polarity due to dispersal of cationic charge by an orbital overlap between metal and ligands. This decline in the polarity of metallic ion augments the lipophilicity of complex leading to high penetration of microbial cell membrane.<sup>42–44</sup> Thus, metal complex can cause the deactivation of variegated cellular enzymes which play a crucial role in metabolic processes of these microbes.

### 3.5 Determination of cytotoxicity

The evaluation of anti-proliferative activity was done by employing MTT assay [3-(4,5-Dimethylthiazol-2-yl)-2, 5-diphenyl tetrazolium bromide] as a screening technique against the PANC-1 cell line.<sup>45</sup> This droid colorimetric analysis is very rapid as well as quantitative and results in the detection of only living cells and can be read on a microplate reader. The signal generated serves as an indication of the number of viable cells. The experiment was performed with varying concentrations of complexes as stated below in Figures 4 and 5. Gemcitabine was used as a positive control.

The complex **1** has demonstrated significantly reduced cell survival rate and high cytotoxicity even at lower concentrations and resulted in an IC<sub>50</sub> value of 18.51  $\mu$ M as illustrated in Figure 4. The cytotoxic potential of complex **1** is dependent upon concentration as the survival rate of malignant cells falls with increase in the concentration of complex **1**.

Complex **2** manifested 50% cytotoxic activity at 2252.8  $\mu$ M. Thus, it can kill the cancerous cells only at higher concentrations.

As evident from the graphs, the anti-cancerous potential of complex **2** is lesser in comparison to that of complex **1**. Hence, complex **1** was tested for its cytotoxic activity on the normal pancreatic cells as can be observed in Figure 6. No significant cytotoxicity of the complex **1** was reported after 24 h with the tested concentrations on the normal, non-transformed hTERT-HPNE cells. Hence, complex **1** can be

**Table 4.** Diameter of inhibition zone.

Sl. no.	Microorganisms	Rifampicin (mm)	Concentration (mg/mL)	Complex 1	Complex 2
A	<i>E. coli</i>	37.6	5.0	20.6 mm	20 mm
B	<i>S. aureus</i>	40	5.0	0	0
C	<i>P. aeruginosa</i>	34	5.0	19 mm	18.3 mm
D	<i>E. hirae</i>	18	5.0	0	0

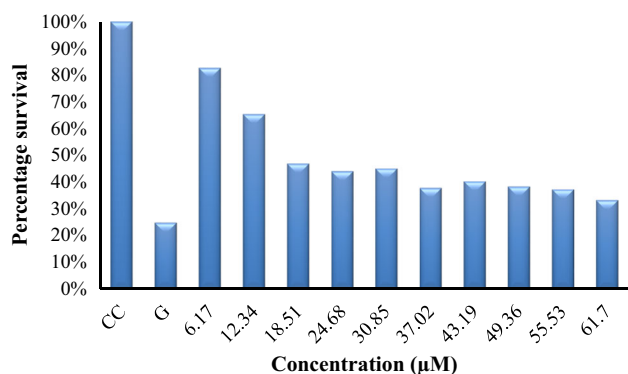


**Figure 4.** Cytotoxic effect of different concentrations (6.17–61.7 μM) of complex **1** on the PANC-1 cancerous cell line after 24 h. CC: Cell Control, G: Gemcitabine. The results were expressed as Mean ± SD of % cell survival from the triplicate experiments.

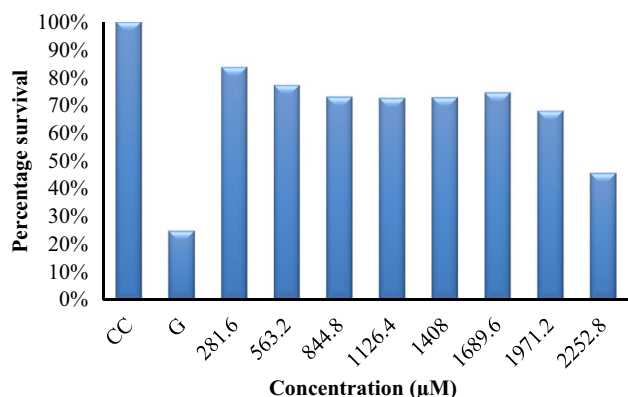


**Figure 5.** Cytotoxic effect of different concentrations (281.6–2252.8 μM) of complex **2** on the PANC-1 cancerous cell line after 24 h. CC: Cell Control, G: Gemcitabine. The results were expressed as Mean ± SD of % cell survival from the triplicate experiments.

considered as an effective and safe candidate for further cytotoxic studies.

#### 4. Conclusions

Two complexes  $[\text{Co}(\text{trien})(\text{NO}_2)_2]_2\text{Cr}_2\text{O}_7$  and  $[\text{Co}(\text{trien})(\text{NO}_2)_2]\text{SCN}$  were synthesized and characterized by physical and spectroscopic methods. Non-covalent interactions such as electrostatic attractions and H-bond interactions such as (trien)  $\text{N}-\text{H}\cdots\text{O}$  ( $\text{Cr}_2\text{O}_7^{2-}$ ) and (trien)  $\text{C}-\text{H}\cdots\text{O}$  ( $\text{Cr}_2\text{O}_7^{2-}$ ),  $\text{N}-\text{H}_{\text{trien}}\cdots\text{N}$  (thiocyanate) and  $\text{C}-\text{H}_{\text{trien}}\cdots\text{N}$  (thiocyanate) stabilized the crystal lattice. The complex **1** and **2** manifested good antibacterial activity against gram negative bacteria displaying zone of growth inhibition of 20.6 mm and 20 mm (*E. coli*) and 19 mm and 18.3 mm

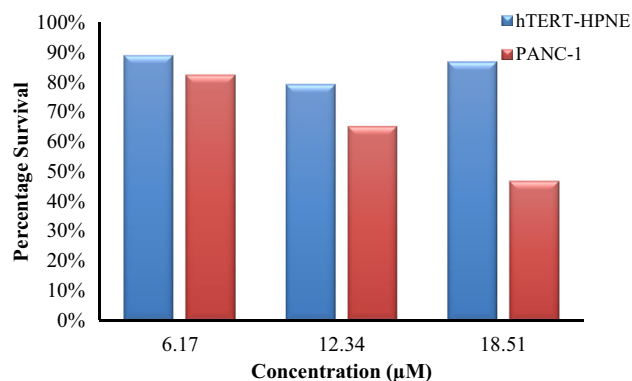


**Figure 6.** Cytotoxic effect of different concentrations (6.17–18.51 μM) of complex **1** on both non-malignant, untransformed normal cells (hTERT-HPNE) and malignant PANC-1 cells after 24 h treatment. The results were expressed as Mean ± SD of % cell survival from the triplicate experiments.

(*P. aeruginosa*), respectively. Tremendous cytotoxic activity against PANC-1 cells was exhibited by the complex **1** even at lower concentration evincing that it could be utilized for the treatment of cancerous cells. However, the cytotoxic potential of complex **2** against the same category of cells is lesser than that of complex **1**. Also, complex **1** did not show any significant cytotoxic effect on the normal cells and can be considered a potent and safe anticancer candidate.

#### Supplementary Information (SI)

Supplementary crystallographic data for structural investigation of the complex  $[\text{Co}(\text{trien})(\text{NO}_2)_2]_2\text{Cr}_2\text{O}_7$  and  $[\text{Co}(\text{trien})(\text{NO}_2)_2]\text{SCN}$  can be acquired free of cost from the Cambridge Crystallographic Data Centre on citing the Deposition number 1951784 and 2014888, respectively. Figures S1–S8 are available at [www.ias.ac.in/chemsci](http://www.ias.ac.in/chemsci).

#### Acknowledgements

Dr. Talwar is very thankful to the DST-FIST for providing single-crystal X-ray facility as well as UGC-CAS's assistance at Panjab University, Chandigarh-160014. He also pays special thanks to the Principal of DAV College, Sector-10, Chandigarh-160010.

#### References

- Busschaert N, Caltagirone C, Rossom W V and Gale P A 2015 Applications of supra molecular anion recognition *Chem. Rev.* **115** 8038
- King R B 1970 Some applications of metal carbonyl anions in the synthesis of unusual organometallic compounds *Acc. Chem. Res.* **3** 417

- Phipps R J, Hamilton G L and Toste F D 2012 The progression of chiral anions from concepts to applications in asymmetric catalysis *Nat. Chem.* **4** 603
- Malabanan M M, Amyes T L and Richard J P 2010 A role for flexible loops in enzyme catalysis *Curr. Opin. Struct. Biol.* **20** 702
- Bilaničová D, Salis A, Ninham B W and Monduzzi M 2008 Specific anion effects on enzymatic activity in nonaqueous media *J. Phys. Chem. B* **112** 12066
- Planells-Cases R and Jentsch T J 2009 Chloride channelopathies *Biochim. Biophys. Acta* **1792** 173
- Quinton P M 2008 Cystic fibrosis: impaired bicarbonate secretion and mucoviscidosis *Lancet* **372** 415
- Beer P D and Gale P A 2001 Anion Recognition and Sensing: The State of the Art and Future Perspectives *Angew. Chem. Int. Ed.* **40** 486
- Zieliński T, Dydio P and Jurczak J 2008 Synthesis, structure and the binding properties of the amide-based anion receptors derived from 1*H*-indole-7-amine *Tetrahedron* **64** 568
- Matthews S E and Beer P D 2005 Calixarene-based anion receptors *Supramol. Chem.* **17** 411
- Saha I, Lee J T and Lee C-H 2015 Recent advancements in Calix[4]pyrrole-based anion-receptor chemistry *Eur. J. Org. Chem.* **18** 3859
- Amendola V, Fabbrizzi L and Mosca L 2010 Anion recognition by hydrogen bonding: urea-based receptors *Chem. Soc. Rev.* **39** 3889
- Byrne S and Mullen K M 2017 Urea and thiourea based anion receptors in solution and on polymer supports *Supramol. Chem.* **30** 196
- Blondeau P, Segura M, Pérez-Fernández R and de Mendoza J 2007 Molecular recognition of oxoanions based on guanidinium receptors *Chem. Soc. Rev.* **36** 198
- Kilah N L and Beer P D 2010 Pyridine and pyridinium-based anion receptors *Top Heterocycl. Chem.* **24** 301
- Llinares J M, Powell D and Bowman-James K 2003 Ammonium based anion receptors *Coord. Chem. Rev.* **240** 57
- Choudhary V R, Patil N S, Chaudhari N K and Bhargava S K 2004 Biphasic selective epoxidation of styrene by *t*-butyl hydroperoxide to styrene oxide using potassium chromate or dichromate catalyst in aqueous medium *Catal. Commun.* **5** 205
- Feiz M and Norouzi H 2014 Dyeing studies of wool fibers with madder (*Rubia Tinctorum*) and effects of different mordants and mordanting procedures on color characteristics of dyed samples *Fiber. Polym.* **15** 2504
- Levis A G and Buttignol M 1977 Effects of potassium dichromate on DNA synthesis in hamster fibroblasts *Br. J. Cancer* **35** 496
- Agbai O 1986 Anti-sickling effect of dietary thiocyanate in prophylactic control of sickle cell anemia *J. Natl. Med. Assoc.* **78** 1053
- Chandler J D and Day B J 2012 Thiocyanate: a potentially useful therapeutic agent with host defense and antioxidant properties *Biochem. Pharmacol.* **84** 1381
- Laurberg P, Pedersen I B, Carlé A, Anderden S, Knudsen N and Karmisholt J 2009 *Comprehensive Handbook of Iodine* (Cambridge: Academic Press) p. 275
- Ambika S, Manojkumar Y, Arunachalam S, Gowdhani B, Sundaram K K M, Solomon R V, Venuvanalingam P, Akbarsha M A and Sundararaman M 2019 Biochemical interaction, anti-cancer and anti-angiogenic properties of cobalt(III) schiff base complexes *Sci. Rep.* **9** 1
- Munteanu C R and Suntharalingam K 2015 Advances in cobalt complexes as anticancer agents *Dalton Trans.* **44** 13796
- Savithri K, Kumar B C V, Vivek H K and Revanasiddappa H D 2018 Synthesis and characterization of cobalt(III) and copper(II) complexes of 2-((E)-(6-Fluorobenzo[d]thiazol-2-ylimino)methyl)-4-chlorophenol: DNA binding and nuclease studies—SOD and antimicrobial activities *Int. J. Spectrosc.* **2018** 1
- McClure M 2008 Synthesis and symmetry of two cobalt(III) complexes with tetradentate ligands *J. Chem. Edu.* **85** 420
- Sheldrick G M 2008 A short history of SHELX *Acta Cryst. A* **64** 112
- Prabst K, Engelhardt H, Ringgeler S and Hubner H 2017 Basic colorimetric proliferation assays: MTT, WST and resazurin *Methods Mol. Biol.* **1601** 1
- Law B Y K, Qu Y Q, Mok S W F, Liu H, Zeng W, Han Y, Gordillo-Martinez F, Chan W-K, Wong K M-C and Wong V K W 2017 New perspectives of cobalt tris(bipyridine) system: anti-cancer effect and its collateral sensitivity towards multidrug-resistant (MDR) cancers *Oncotarget* **8** 55003
- Thamilarasan V, Sengottuvelan N, Sudha A, Srinivasan P and Chakkaravarthi G 2016 Cobalt(III) complexes as potential anticancer agents: physicochemical, structural, cytotoxic activity and DNA/protein interactions *J. Photochem. Photobiol. B* **162** 558
- Buckingham D A and Jones D 1965 Infrared spectra of cobalt(III) triethylenetetramine complexes *Inorg. Chem.* **4** 1387
- Al-Kayssi M and Magee R I 1962 Analytical applications of infrared spectroscopy identification of polyatomic inorganic anions *Talanta* **9** 667
- Sharma R P, Sharma R, Bala R, Salas J M and Quiros M 2006 Second sphere coordination complexes via hydrogen bonding: synthesis, spectroscopic characterization of  $[trans-Co(en)_2Cl_2]CdX_4$  (X = Br or I) and single crystal X-ray structure determination of  $[trans-Co(en)_2Cl_2]CdBr_4$ , *J. Mol. Struct.* **794** 341
- Fuziwara T and Bailar J C 1988 Reactions of coordination compounds in the solid state II. The interconversion of the isomers of dichloro(triethylenetetramine)cobalt(III) chloride,  $[Co(trien)Cl_2]Cl$ , upon heating in the solid state *Bull. Chem. Soc. Jpn.* **61** 849
- McClure M R and Holcombe J 2004 Synthesis and NMR characterization of cobalt(III) complexes with triethylenetetramine, 2,2-bipyridine and 1,10-phenanthroline *J. Coord. Chem.* **57** 907
- Sargeson A M and Searle G H 1967 The stereochemistry and preparation of triethylenetetramine-disubstituted cobalt(III) complexes *Inorg. Chem.* **6** 787
- Pecile C 1966 Infrared studies of planer and tetrahedral inorganic thiocyanates *Inorg. Chem.* **5** 210
- Derwahl A, Dickie A J, House D A, Jackson W G, Schaffner S, Svensson J, Turnbull M M and Zehnder

- M 1997 Anionopentaaminecobalt(III) complexes with polyamine ligands 28. The crystal structure of [CoCl(tacn)(en)]ZnCl<sub>4</sub>, [CoCl(tacn)(ampy)] ZnCl<sub>4</sub>.H<sub>2</sub>O, unsym-[CoCl(N-Metacn)(en)]-ZnCl<sub>4</sub>.H<sub>2</sub>O, *trans*-(R,S)-[CoCl(2,2,3-tet)(NH<sub>3</sub>)] ZnCl<sub>4</sub> and unsym-*fac*-[CoCl(bn)(dien)] ZnCl<sub>4</sub> *Inorg. Chim. Acta* **257** 179
39. Guzei I A and Arderne C 2015 Polymorphism of dinitro[tris(2-aminoethyl)amine]-cobalt(III) chloride *Acta Crystallogr. C* **71** 695
40. House D A and Svensson J 1998 Kinetic studies using Co(III) and Cr(III) complexes of 1,4,7,11-tetraazaundecane (2,2,3-tet) and the crystal structure of *trans*-[CrCl<sub>2</sub>(2,2,3-tetH)(OH<sub>2</sub>)]Cl.ClO<sub>4</sub> *Inorg. Chim. Acta* **278** 24
41. Khranenko S P, Kuratieva N V, Korolkov I V and Gromilov S A 2016 Crystal structure of [Pb<sub>3</sub>(OH)<sub>4</sub>.Co(NO<sub>2</sub>)<sub>3</sub>](NO<sub>3</sub>)(NO<sub>2</sub>).2H<sub>2</sub>O *J. Struct. Chem.* **57** 625
42. Arora S, Talwar D, Singh M, Sahoo S C and Sharma R 2019 Second sphere coordination in orthonitrophenolate binding: synthesis, biological, cytotoxic and X-ray structural studies of [Co(bpy)<sub>2</sub>CO<sub>3</sub>](C<sub>6</sub>H<sub>4</sub>NO<sub>3</sub>).3H<sub>2</sub>O *J. Mol. Struct.* **1199** 127017
43. Kumar R S and Arunachalam S 2008 Synthesis, micellar properties, DNA binding and antimicrobial studies of some surfactant-cobalt(III) complexes *Biophys. Chem.* **136** 136
44. Chang E L, Simmers C and Knight D A 2010 Cobalt complexes as antiviral and antibacterial agents *Pharmaceuticals* **3** 1711
45. Kumar R S, Arunachalam S, Periasamy V S, Preethy C P, Riyasdeen A and Akbarsha M A 2009 Surfactant-cobalt(III) complexes: synthesis, critical micelle concentration (CMC) determination, DNA binding, antimicrobial and cytotoxicity studies *J. Inorg. Biochem.* **103** 117